Available online at www.sciencedirect.com
SCIENCE DIRECT®
Dyes and Pigments 69 (2006) 210–223
DYES and PIGMENTS
www.elsevier.com/locate/dyepig

Removal of Orange-G and Methyl Violet dyes by adsorption onto bagasse fly ash—kinetic study and equilibrium isotherm analyses

Indra D. Mall *, Vimal C. Srivastava, Nitin K. Agarwal

Department of Chemical Engineering, Indian Institute of Technology Roorkee, Roorkee – 247667, India

Received 19 December 2004; received in revised form 12 January 2005; accepted 18 March 2005
Available online 25 May 2005

Abstract

In the study, bagasse fly ash (BFA) (generated as waste material from sugar mill), was used as an adsorbent for the removal of Orange-G (OG), and Methyl Violet (MV), from aqueous solution. Batch studies were performed to address various experimental parameters like pH, contact time, adsorbent dose and initial concentration for the removal of these dyes. Effective pH for OG and MV removal were 4 and 9, respectively. Greater percentage of dye was removed with decrease in the initial concentration of dyes, and increase in amount of adsorbent used. Kinetic study showed that the adsorption of dyes on BFA was a gradual process. Quasi-equilibrium reached in 4 h. Pseudo-first-order, pseudo-second-order, Bangham and intra-particle particle diffusion models were used to fit the experimental data. Pseudo-second-order rate equation was able to provide realistic description of adsorption kinetics. Equilibrium isotherms were analysed by Freundlich, Langmuir, Redlich–Peterson, Dubnin–Radushkevich, and Tempkin isotherm equations using correlation coefficients and five different error functions. Freundlich equation is found to best represent the equilibrium data for OG-BFA system while Redlich–Peterson equation better fits the data for MV-BFA system. Thermodynamic study showed that adsorption of MV on BFA (with a more negative Gibbs free energy value) is more favoured among the dyes studied. BFA which was used without any pretreatment showed high surface area, pore volume and pore size exhibiting its potential to be used as an adsorbent for the removal of OG and MV.

Keywords: Adsorption; Dye removal; Bagasse fly ash; Kinetic study; Error analyses

1. Introduction

Colour is the most obvious indicator of water pollution. The discharge of coloured wastes into receiving streams not only affects the aesthetic nature but also interferes with transmission of sunlight into streams and therefore reduces photosynthetic activity [1]. Dyes and pigments represent one of the problematic groups; they are emitted into wastewaters from various industrial branches, mainly from the dye manufacturing and textile finishing. Dyes can be classified as anionic (direct, acid, and reactive dyes), cationic (basic dyes) and non-ionic (disperse dyes) [2]. Wastewaters offer considerable resistance for their biodegradation due to presence of these heat and light stable dyes, thus upsetting aquatic life [3]. Hence, the conventional methods used in sewage treatment, such as primary and secondary treatment systems, are unsuitable [4]. The adsorption process provides an attractive alternative treatment, especially if the adsorbent is inexpensive and readily available. Granular activated carbon is the most

* Corresponding author. Tel.: +91 1332 285319 (O), 285106 (R); fax: +91 1332 276535, 273560.
E-mail address: id_mall2000@yahoo.co.in (I.D. Mall).

0143-7208/$ - see front matter © 2005 Elsevier Ltd. All rights reserved.
doi:10.1016/j.dyepig.2005.03.013

popular adsorbent and has been used with great success [5], but is expensive. Consequently, many investigators have studied the feasibility of using low cost substances, such as: plum kernels [6], chitin [7], chitosan [8], perlite [9], natural clay [10–12], bagasse pith [13–15], coal fly ash [16], boiler bottom ash [17], bagasse fly ash [18,19], wood [20–24], rice husk [25], peat [26–28], maize cob [29], bean waste [30], banana pith [31–33], coir pith [34,35], red mud [36], orange peel [37], biogas waste slurry [38,39] as adsorbents for the removal of dyes from wastewaters. Critical review of low cost adsorbents for waste and wastewater treatment has been presented by Pollard et al. [40], Mall et al. [41], and Bailey et al. [42].

Bagasse fly ash (BFA) is a waste obtained from the bagasse fired boiler stack of cane sugar mills. The BFA is currently being used as filler in building materials. It has been used previously for the COD removal form sugar mill [43] and paper mill effluents [44]. Various researchers have utilized it for the adsorptive removal of phenolic compounds [45,46], metals [47,48] and dyes [49]. But from the survey of the literature, no information for the adsorptive removal of Orange-G (OG) and Methyl Violet (MV) by BFA is available. Thus, the main objects of this paper are: (i) to study the feasibility of using BFA as an adsorbent for the removal of OG and MV dyes, (ii) to determine the physico-chemical characteristics and thermal stability of BFA, (iii) to determine the various parameters affecting sorption, such as pH, adsorbent dose, initial concentration, contact time, (iv) to evaluate the usefulness of various kinetic models, viz. pseudo-first-order, pseudo-second-order, Bangham and intra-particle diffusion models, and (v) to determine the applicability of various isotherm models (i.e., Freundlich, Langmuir, Redlich–Peterson, Dubinin and Radushkevich, and Tempkin) based on the error analysis using five different error analysis techniques to find out the best-fit isotherm equation.

2. Material and methods

2.1. Bagasse fly ash (BFA) and its characterization

Low cost adsorbent BFA was used as such without any pretreatment except for the sieving of very fine particles for the present study. Physico-chemical characteristics of the BFA were determined using standard procedures. Proximate analysis was carried out using the procedure as per IS standards [50]. Bulk density was determined by using MAC bulk density meter whereas particle size analysis was done using standard sieve. X-ray diffraction analysis of BFA was carried out using Phillips (Holland) diffraction unit (Model PW 1140/90), using copper target with nickel as filter media, and K radiation maintained at 1.542 Å. Goniometer speed was maintained at 1°/min. Thermal analysis was used to ascertain the thermal stability of the adsorbents. Although many different thermal techniques are commonly used, in the present report we will refer exclusively to thermogravimetric analysis (TGA), differential thermal analysis (DTA), and derivative thermogravity (dTG). The thermal analysis (TGA, DTA and dTG) of BFA was performed using a Perkin–Elmer Pyris Diamond TG/TGA instrument at a fixed heating rate of 20 K/min over a temperature range of 25–1000 °C using alumina powder (10.5 mg) as reference. BFA sample of ~10 mg was uniformly spread over the balance pan. The degradation runs were taken under an inert atmosphere (flowing nitrogen) for pyrolysis and an oxidizing atmosphere (flowing dry air) for gasification at a flow rate of 100 ml/min.

2.2. Adsorbates

A.R. grade Orange-G (OG) and Methyl Violet (MV) dyes supplied by Aldrich Chemical Co. (USA) were used as adsorbate in the present study. The characteristics and chemical structures of these dyes are listed in Table 1 and Fig. 1, respectively. Methyl Violet contains a secondary amine group. The colour of Methyl Violet changes from yellow to green in the pH range 0.13–0.50, from green to blue in the pH range 2.0–3.0. When pH is higher than 3, the solubility of Methyl Violet is essentially unchanged. Accurately weighed quantities of dyes were dissolved in distilled water to prepare stock solutions of the dyes. Since MV dye is difficult to dissolve in water, the dye solution was allowed to stand for one day until the absorbance of the solutions remained unchanged. Experimental solutions of desired dye concentration were obtained by successive dilutions.

2.3. Analytical measurements

Concentrations of dyes were determined by finding out the absorbance characteristic wavelength using UV-spectrophotometer (Schimadzu, Japan). A standard solution of the dye was taken and the absorbance was determined at different wavelengths to obtain a plot of absorbance versus wavelength. The wavelength corresponding to maximum absorbance (λ_{max}) was determined from this plot. The λ_{max} for OG and MV were found to be 476 and 580 nm, respectively. Calibration curves were plotted between absorbance and concentration of the dye solution.

2.4. Batch experimental programme

To study the effect of important parameters batch experiments were conducted. For each experimental run, 50 ml of dye of known concentration, pH and the known amount of the BFA were taken in a 100 ml stoppered conical flask. This mixture was agitated in

Table 1
The physical and chemical characteristics of dyes

Dye name	Abbreviation	Generic name	λ_{max} (nm)	C.I.	Chemical formula	F.W.
Orange-G	OG	Acid orange 10	476	16230	$C_{16}H_{10}N_2Na_2O_7S_2$	452.36
Methyl Violet	MV	Basic violet 1	580	42535	$C_{24}H_{28}ClN_3$	393.95

a temperature controlled by shaking water bath at a constant speed of 150 revolutions per minutes (rpm) at 30 ± 1 °C. Samples were withdrawn at appropriate time intervals and supernatant liquid portions centrifuged using Research Centrifuge (Remi scientific works Mumbai), at 5 000 rpm for 20 min and analysed for remaining dye concentration spectrophotometrically using UV-spectrophotometer (Schimadzu, Japan). Experiments were carried out at initial pH values ranging from 3 to 12; initial pH was controlled by the addition of dilute HCI or NaOH solutions.

The percentage of removal of dyes and equilibrium adsorption uptake, q_e (mg/g), was calculated using the following relationships:

$$\text{Percentage removal} = 100(C_0 - C_e)/C_0, \quad (-) \tag{1}$$

$$\text{Amount adsorbed } q_e = (C_0 - C_e)V/w, \quad (\text{mg of adsorbate/g of adsorbent}) \tag{2}$$

where C_0 is the initial sorbate concentration (mg/l), C_e is the equilibrium sorbate concentration (mg/l), V is the volume of the solution (l) and w is the mass of the adsorbent (g).

For optimum amount of BFA per unit mass adsorbate, a 50 ml dye solution was contacted with different amounts of BFA till equilibrium was attained. Kinetics of adsorption was determined by analyzing adsorptive uptake of the dye from aqueous solution at different time intervals. For adsorption isotherms, dye solutions of different concentrations were agitated with known amount of BFA till the equilibrium was achieved. The residual dye concentration was then determined. Blank runs, with only the BFA in 50 ml of double-distilled water, were conducted simultaneously at similar conditions to account for any colour leached by the BFA and adsorbed by glass containers.

3. Results and discussion

3.1. Characterization of adsorbents

Characteristics of BFA determined included, bulk density, particle size, and proximate analysis. The particle sizes of BFA were <180 (31.71%), 180–212 (39.92%), 212–850 (21.95%), 850–1000 (1.97%), 1000–1180 (2.09%), 1180–1400 (1.40%) and >1400 (0.96%) μm. Moisture content, volatile matter, ash, fixed carbon and bulk density of BFA were 7.64%, 17.37%, 26.43%, 48.56% and 133.3 kg/m^3, respectively. For structural and morphological characteristics, scanning electron microscope analysis and X-ray diffraction were carried out. Scanning electron microscopic photograph (Fig. 2) of BFA reveals surface texture and porosity. This photomicrograph shows fibrous structure of BFA. d-spacing values provided by the X-ray

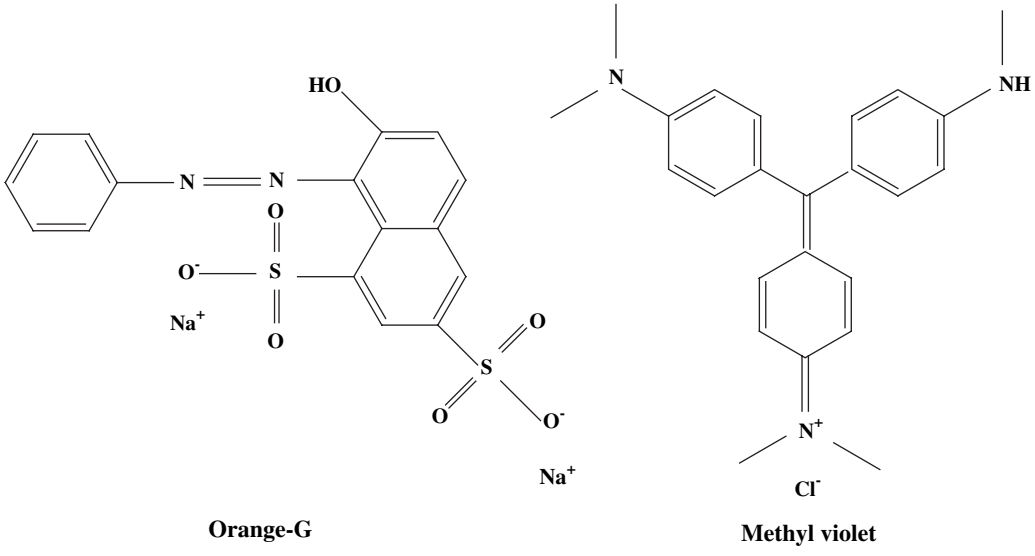

Fig. 1. Molecular structures of the dyes.

Fig. 2. Scanning electron micrograph of bagasse fly ash.

spectrum of BFA reflects the presence of alumina (Al_2O_3), silica (SiO_2), CaO, $CaSiO_3$, and $Ca_8Si_5O_{18}$. Diffraction peaks corresponding to crystalline carbon were not observed in BFA.

3.1.1. Thermal stability of BFA

Thermal stability of BFA is directly dependent on the decomposition temperature of its various oxides and functional groups. The surface groups present on carbons and those formed as a result of interaction with oxidizing gases or solutions are generally quite stable even under vacuum at temperatures below 150 °C, irrespective of the temperature at which they were formed. However, when the carbons are heated at higher temperatures, the surface groups decompose, producing CO (200–600 °C), CO_2 (450–1000 °C) [51], water vapour and free hydrogen (500–1000 °C).

The thermogravimetric analysis curves (TGA, DTA and dTG) of BFA under inert and oxidizing atmosphere are shown in Fig. 3. Three different zones can be envisaged: from room temperature to ca. 400 °C, from 400 to 530 °C and from 530 to 1000 °C. Main weight loss was recorded in the second zone, while first and third zone correspond to comparatively small weight losses.

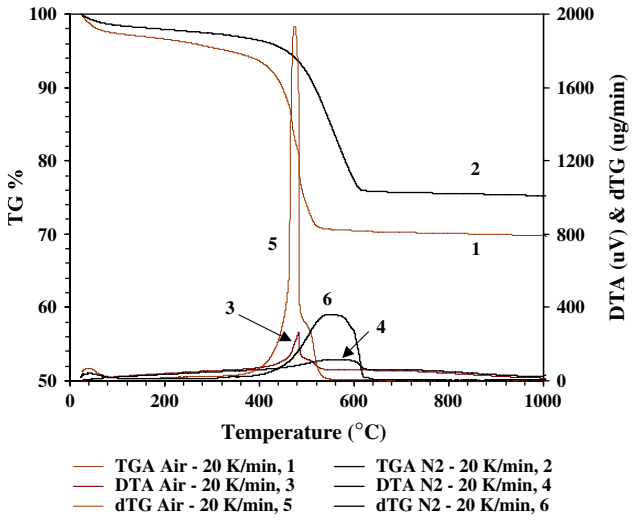

Fig. 3. TGA, DTA and dTG plots for BFA.

Under air atmosphere, first zone corresponds to removal of moisture and light volatiles up to 370 °C with a total loss of about 6.4%. This initial zone is followed by the active pyrolysis and oxidation zone from 370 °C to 528 °C with total degradation of 22.8%. Subsequently, the sample weight remains almost constant with total degradation of 1.1% up to 1000 °C. The residue left at 1000 °C is ash and is about 70% of the original sample weight. Thermal degradation characteristics in flowing nitrogen atmosphere shows removal of moisture and light volatiles of about 4.8% up to temperature of 450 °C followed by an active pyrolysis zone between 450 and 625 °C. Total degradation during this zone is about 19.2%. Beyond 625 °C, the sample weight almost remains constant. The residue left at 1000 °C is the weight of the char and is equal to the 76% of the initial sample weight. BFA does not show any endothermic transition between room temperature and 300 °C, indicating the lack of any crystalline or other phase change during the heating process [52]. The strong exothermic peak centered around 480 °C is due to the oxidative degradation of the sample. This broad as also observed from first derivative loss curve (dTG) shown in Fig. 3 may be due to the combustion of carbon species. At higher temperatures (third zone), the samples present a gradual weight loss up to 800 °C. This weight loss has been reported to be associated in part with the evolution of CO_2 and CO. Finally no mass loss was detected when temperature was increased up to 1000 °C. This result indicates the presence of oxides (mainly those of silicon and aluminum), which are stable at higher temperatures.

3.2. Effect of pH

The pH of the solution affects the surface charge of the adsorbents as well as the degree of ionization of

different pollutants. The hydrogen ion and hydroxyl ions are adsorbed quite strongly and therefore the adsorption of other ions is affected by the pH of the solution. Change of pH affects the adsorptive process through dissociation of functional groups on the adsorbent surface active sites. This subsequently leads to a shift in reaction kinetics and equilibrium characteristics of adsorption process.

The adsorption of OG and MV by BFA was studied over a pH range of 3–12 at 30 °C and the studies were carried out for 5 h. Initial dye concentration was 10 mg/l and the adsorbent dose was kept at 0.1 and 0.2 g/50 ml for OG and MV, respectively. Fig. 4 shows that the effect of pH on the adsorptive removal of OG and MV by BFA. The percentage removal of OG (anionic dye) was maximum at acidic pH (pH 3–4) and decreased with further increase in pH. In the aqueous solution, the acid dye is first dissolved and the sulphonate groups of the acid dye ($D-SO_3Na$) are dissociated and converted to anionic dye ions.

$$D-SO_3Na \xrightarrow{H_2O} D-SO_3^- + Na^+$$

The oxides of alumina, calcium, silica etc. present in the BFA develop positive charge in contact with water. Except silica, all other oxides possess positive charge for the pH range of interest because zero point charge of SiO_2, Al_2O_3 and CaO are 2.2, 8.3 and 11.0, respectively [53]. The negatively charged silica sites of adsorbent get neutralized by H^+ ions thereby reducing hindrance to diffusion of anionic dye ions. For pH below 4, a significantly high electrostatic attraction exists between the positively charged surface of the adsorbent and anionic dye. As the pH of the system increased, the number of negatively charged sites increased and the number of positively charged sites decreased. A negatively charged surface site on the adsorbent did not favour the adsorption of dye anions due to electrostatic repulsion. Also, there was competition between OH^- (at high pH) and coloured ions of OG for positively charged adsorption sites. The trend was similar to the adsorption of acid violet and acid brilliant blue on waste coir pith [34].

Percentage of removal of MV (cationic dye) increased with increase in pH. As the pH of dye solution became higher, the association of dye cations with more negative charged site could easily take place thereby increasing its removal.

$$MO^- + Dye^+ \rightleftharpoons M-O-Dye$$

where M stands for alumina, calcium, silica etc. present in the BFA. Higher removal of MV in the alkaline pH range has been reported by other workers also [9,18]. Further experiments were carried out at optimum pH of 4 and 9 for OG and MV, respectively.

3.3. Effect of BFA dosage and initial dye concentration

The effect of BFA dosage on removal of various dyes is shown in Fig. 5. The percentage removal increased with the BFA dosage up to a certain limit and then it reached a constant value. Optimum BFA dosages for OG and MV removal were 0.1 and 0.2 g of BFA per 50 ml of solution, respectively. The increase in adsorption of dyes with adsorbent dosage was due to the availability of more surface area of the BFA for adsorption.

A given mass of adsorbent can adsorb only a fixed amount of adsorbate. So the initial concentration of adsorbate solution is very important. The effect of initial OG and MV dye concentrations for their removal by BFA is shown in Fig. 6. From the figure, it is evident that higher percentage of dye was removed with decrease in initial dye concentration for all the dyes. However, the amount of dye adsorbed per unit adsorbent mass increased with increase in initial dye concentration due to the decrease in resistance to the uptake of solute from solution of dye.

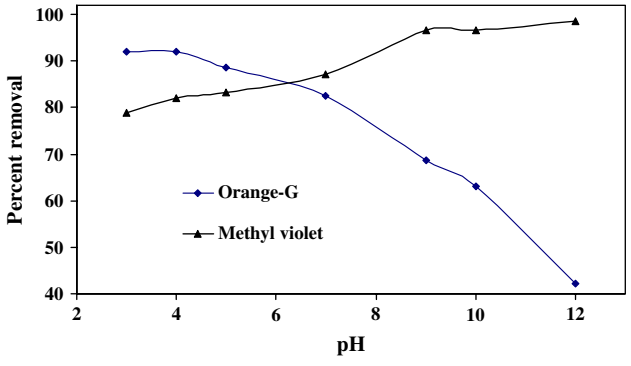

Fig. 4. Effect of pH on the adsorption of dyes by BFA (temperature = 30 °C, contact time = 300 min, initial dye concentration = 10 mg/l, BFA dosage = 0.1 g/50 ml (OG); 0.2 g/50 ml (MV)).

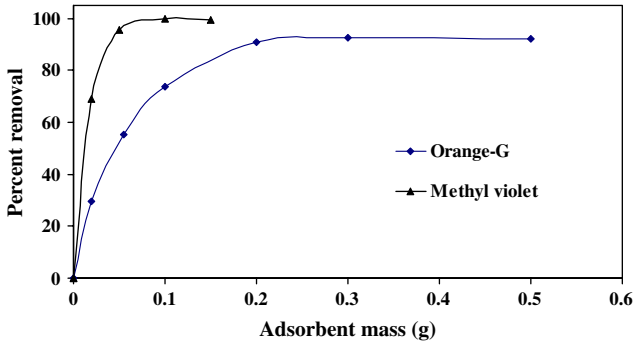

Fig. 5. Effect of adsorbent mass on the adsorption of dyes by BFA (temperature = 30 °C, contact time = 300 min, volume of sample = 50 ml, initial dye concentration = 10 mg/l).

3.4. Effect of contact time

The contact time between the pollutant and the adsorbent is of significant importance in the wastewater treatment by adsorption. A rapid uptake of pollutants and establishment of equilibrium in a short period signifies the efficacy of that adsorbent for its use in wastewater treatment. In physical adsorption most of the adsorbate species are adsorbed within a short interval of contact time. However, strong chemical binding of the adsorbate with adsorbent requires a longer contact time for the attainment of equilibrium. Available adsorption studies in literature reveal that the uptake of adsorbate species is fast at the initial stages of the contact period, and thereafter, it becomes slower near the equilibrium. In between these two stages of the uptake, the rate of adsorption is found to be nearly constant. This is obvious from the fact that a large number of vacant surface sites are available for adsorption during the initial stage, and after a lapse of time, the remaining vacant surface sites are difficult to be occupied due to repulsive forces between the solute molecules on the solid and bulk phases.

The effect of contact time for the adsorption of OG and MV by BFA was studied for a period of 24 h for initial dye concentrations of 10 mg/l at 30 °C. BFA dosage was 0.1 and 0.2 g/50 ml of dye solution for OG and MV, respectively, at respective optimum pH. Dye solutions were kept in contact with BFA for 24 h although no significant variation in residual dye concentration was detected after 4 h of contact time. Thus, after 4 h of contact, a steady-state approximation was assumed and a quasi-equilibrium situation was accepted. Fig. 7 presents the effect of contact time for first 6 h only. The contact time curve shows that the dye removal was rapid in the first 15 min. The curves of contact time are single, smooth and continuous leading to saturation. These curves indicate the possible monolayer coverage of dye on the surface of BFA [3,25,54]. Pedro Silva et al. [55] have reported 1 h equilibrium contact time for acid orange 7 dye adsorption on spent brewery grains. Similarly a contact time of only about 25 min was required to attain the equilibrium adsorption of dyes to carbonaceous adsorbents [56]. Dogan and Alkan [9] have reported 30 min equilibrium contact time for removal of MV by perlite at 30 °C. As comparison, 4 h quasi-equilibrium contact time for OG and MV adsorption on BFA is much higher. It was also found from Fig. 6 that the percent removal of dyes was in the order MV > OG at any contact time. This trend was observed because MV with smaller size could get adsorbed more deeply into that pore which was big enough not to adsorb much greater size OG dye molecule.

3.5. Adsorption kinetic study

In order to investigate the adsorption processes of OG and MV on BFA, four kinetic models were used, including pseudo-first-order, pseudo-second-order, Bangham and intra-particle diffusion models.

3.5.1. Pseudo-first-order model

The pseudo-first-order equation is

$$\frac{dq_t}{dt} = k_f(q_e - q_t) \tag{3}$$

where q_t is the amount of adsorbate adsorbed at time t (mg/g), q_e is the adsorption capacity in equilibrium (mg/g), k_f is the rate constant of pseudo-first-order model (min^{-1}), and t is the time (min). After definite integration by applying the initial conditions $q_t = 0$ at $t = 0$ and $q_t = q_t$ at $t = t$, the equation becomes [57]:

$$\log(q_e - q_t) = \log q_e - \frac{k_f}{2.303}t \tag{4}$$

Values of adsorption rate constant (k_f) for OG and MV adsorption on BFA were determined from the plot of $\log(q_e - q_t)$ against t (not shown). These values

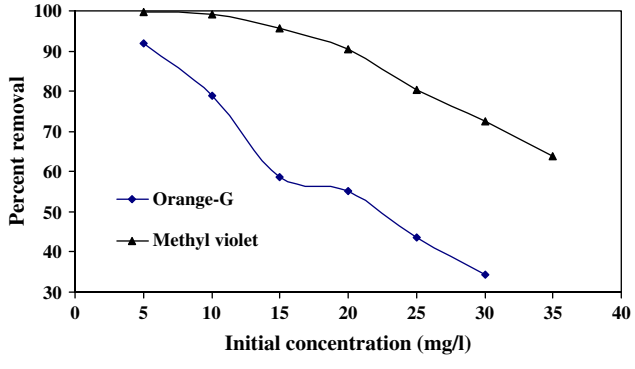

Fig. 6. Effect of initial adsorbate concentration of on removal of dyes by BFA (temperature = 30 °C, contact time = 240 min, BFA dosage = 0.1 g/50 ml (OG); 0.2 g/50 ml (MV)).

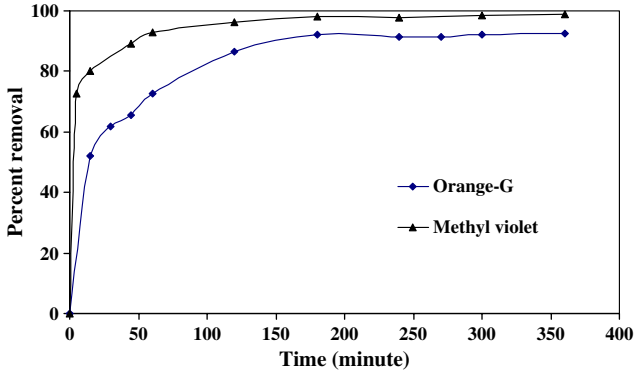

Fig. 7. Effect of contact time on removal of dyes by BFA (temperature = 30 °C, initial dye concentration = 10 mg/l, BFA dosage = 0.1 g/50 ml (OG); 0.2 g/50 ml (MV)).

(Table 2) indicate that the adsorption rate was very fast at the beginning of adsorption and that rate of removal of MV is faster on BFA between the two dyes. Mall and Upadhyay [18] and Dogan and Alkan [9] have reported k_f value of 0.01539 min^{-1} and 0.273 min^{-1} for MV adsorption, respectively, on bottom ash and perlite. These values are close to the values obtained in the present work.

3.5.2. Pseudo-second-order model

The pseudo-second-order model can be represented in the following form [58]:

$$\frac{dq_t}{dt} = k_S(q_e - q_t)^2 \quad (5)$$

where k_S is the rate constant of pseudo-second-order model (in g/mg min). After integrating Eq. (5) for boundary conditions $q_t = 0$ at $t = 0$ and $q_t = q_t$ at $t = t$, the following form of equation can be obtained:

$$\frac{t}{q_t} = \frac{1}{k_S q_e^2} + \frac{1}{q_e} t \quad (6)$$

the initial sorption rate, h (mg/g min), as $t \to 0$ can be defined as

$$h = k_S q_e^2 \quad (7)$$

The initial sorption rate (h), the equilibrium adsorption capacity (q_e), and the pseudo-second-order constant k_S can be determined experimentally from the slope and intercept of plot of t/q_t versus t (Fig. 8). Calculated correlation coefficients, both linear and non-linear, for pseudo-first-order model and pseudo-second-order model by using regression procedure for OG and MV adsorption are shown in Table 2. Since calculated correlation coefficients are closer to unity for pseudo-second-order kinetics model than the pseudo first-order kinetic model, therefore the adsorption kinetics could well be approximated more favourably by pseudo-second-order kinetic model for all the three dyes. The k_S and h values as calculated from the Fig. 8 are listed in Table 2. It can be seen that the initial sorption rate (h value) for adsorption of MV on BFA is highest. Pedro Silva et al. [55] reported a k_S value of 0.04267 g/mg min for acid orange 51 adsorption on activated bleaching earth. Due to different nature of the adsorbate–adsorbent system in the present work, a direct comparison of k_S is not possible.

3.5.3. Bangham's equation

Kinetic data were further used to know about the slow the step occurring in the present adsorption system using Bangham's equation [59].

$$\log\log\left(\frac{C_0}{C_0 - q_t m}\right) = \log\left(\frac{k_0 m}{2.303 V}\right) + \alpha \log(t) \quad (8)$$

where C_0 is the initial concentration of adsorbate in solution (mg/l), V is the volume of solution (ml), m is the weight of adsorbent per liter of solution (g/L), q_t (mg/g) is the amount of adsorbate retained at time t, and α (<1) and k_0 are constants. The double logarithmic plot (Fig. 9) according to above equation did not yielded perfect linear curves (R^2 (non-linear) ≤ 0.9816) for OG and MV removal by BFA showing that the diffusion of adsorbate into pores of the sorbent is not the only rate-controlling step [60].

Table 2
Kinetic parameters for the removal of dyes by bagasse fly ash

Pseudo-first-order constants				
Dye	k_f (min^{-1})	q_e (mg/g)	R_1^2 (linear)	R_2^2 (non-linear)
Orange-G	0.0115	1.245	0.9227	0.9724
Methyl Violet	0.0219	3.712	0.9065	0.9508
Pseudo-second-order constants				
Dye	h (mg/g min)	k_s (g/mg min)	R_1^2 (linear)	R_2^2 (non-linear)
Orange-G	0.5052	0.1275	0.9993	0.9998
Methyl Violet	2.2421	0.0229	0.9997	0.9999
Bangham constants				
Dye	k_0 (ml/(g/l))	α	R_1^2 (linear)	R_2^2 (non-linear)
Orange-G	12.0208	0.2064	0.9687	0.9842
Methyl Violet	10.2589	0.2587	0.9636	0.9816
Intra-particle diffusion constants				
Dye	$k_{id,1}$ (mg/g min)	R_1^2 (non-linear)	$k_{id,2}$ (mg/g min)	R_2^2 (non-linear)
Orange-G	0.1768	0.9989	0.0292	0.9206
Methyl Violet	0.3073	0.9801	0.0601	0.8722

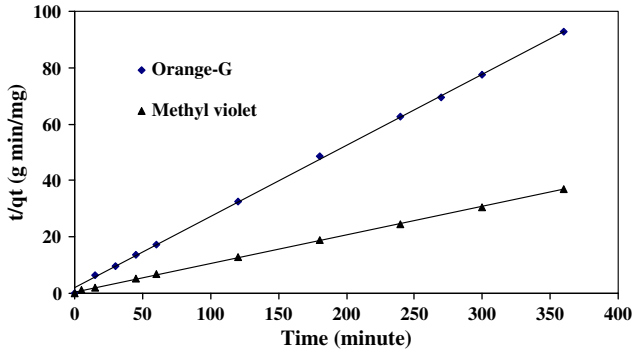

Fig. 8. Pseudo-second-order kinetic plots for removal of dyes by BFA (temperature = 30 °C, contact time = 240 min, initial dye concentration = 10 mg/l, BFA dosage = 0.1 g/50 ml (OG); 0.2 g/50 ml (MV)).

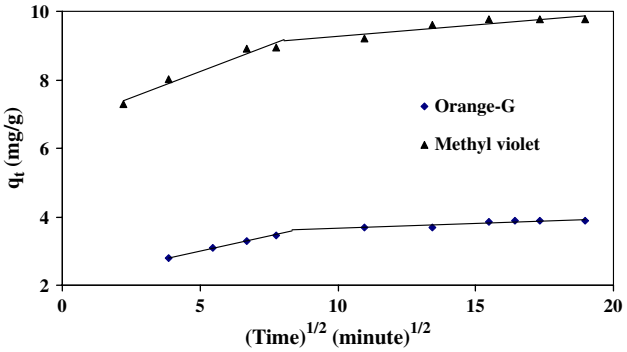

Fig. 10. Weber and Morris intra-particle diffusion plots for removal of dyes by BFA (temperature = 30 °C, contact time = 240 min, initial dye concentration = 10 mg/L, BFA dosage = 0.1 g/50 ml (OG); 0.2 g/50 ml (MV)).

3.5.4. Intra-particle diffusion study

An empirically found functional relationship, common to the most adsorption processes, is that the uptake varies almost proportionally with $t^{1/2}$, the Weber–Morris plot, rather than with the contact time, t [61].

$$q_t = k_{id} t^{1/2} + C \quad (9)$$

where k_{id} is the intra-particle diffusion rate constant. According to Eq. (9), a plot of q_t versus $t^{1/2}$ should be a straight line with a slope k_{id} and intercept C when adsorption mechanism follows the intra-particle diffusion process. Values of intercept give an idea about the thickness of boundary layer, i.e., the larger the intercept the greater is the boundary layer effect [62]. In Fig. 10, plot of mass of dyes adsorbed per unit mass of adsorbent, q_t versus $t^{1/2}$ is presented for OG and MV dyes. The deviation of straight lines from the origin (Fig. 10) may be due to the difference in rate of mass transfer in the initial and final stages of adsorption [53]. Further such deviation of straight line from the origin indicates that the pore diffusion is not the sole rate-controlling step [20] as shown earlier by Bangham's equation. From Fig. 10, it may be seen that there are two separate regions – the first straight portion is attributed to the macropore diffusion (phase I) and the second linear portion to micro-pore diffusion (phase II) [28]. These show only the pore diffusion data. In phase (I), about 62% of OG was uptaken by BFA within a $t^{1/2}$ value of 5.8 min and manifests an average rate of uptake of about 0.565 mg/g min$^{1/2}$. This is attributed to the instantaneous utilisation of the most readily available adsorbing sites on the adsorbent surface. For MV adsorption on BFA, 80% removal took place within a $t^{1/2}$ value of 3.9 min, manifesting an average rate of uptake of about 2.07 mg/g min$^{1/2}$. Phase (II) may be attributed to a very slow diffusion of the adsorbates from the surface film into the micro-pores, which are the least accessible sites of adsorption. This also stimulates a very slow rate of migration of adsorbates from the liquid phase on to the adsorbent surface. The values of $k_{id,1}$ and $k_{id,2}$ as obtained from the slopes of straight lines are listed in Table 2.

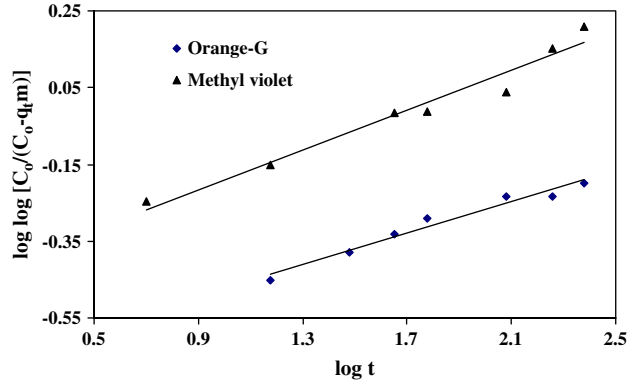

Fig. 9. Bangham plot for removal of dyes by BFA (temperature = 30 °C, contact time = 240 min, initial dye concentration = 10 mg/L, BFA dosage = 0.1 g/50 ml (OG); 0.2 g/50 ml (MV)).

3.6. Adsorption equilibrium study

To optimize the design of an adsorption system for the adsorption of adsorbates, it is important to establish the most appropriate correlation for the equilibrium curves. Various isotherm equations have been used to describe the equilibrium nature of adsorption. Some of these equations are Freundlich, Langmuir, Redlich–Peterson, Dubinin and Radushkevich, Tempkin, Radko–Praunitz and Toth equations.

3.6.1. Freundlich and Langmuir isotherms

Freundlich [63] studied the sorption of a material onto animal charcoal and demonstrated that the ratio of the amount of solute adsorbed onto a given mass of adsorbent to the concentration of the solute in the solution was not a constant at different solution concentrations. The Freundlich isotherm is derived by

assuming a heterogeneous surface with a non-uniform distribution of heat of adsorption over the surface. Langmuir [64] proposed a theory to describe the adsorption of gas molecules onto metal surfaces. The Langmuir adsorption isotherm has been successfully applied to many other real sorption processes and it has been used to explain the sorption of dyes onto various adsorbents. A basic assumption of the Langmuir theory is that sorption takes place at specific homogeneous sites within the adsorbent. It is then assumed that once a dye molecule occupies a site, no further adsorption can take place at that site. Theoretically, therefore, a saturation value is reached beyond which no further sorption can take place. The linearised Freundlich and Langmuir isotherms are represented by the following equations:

$$\text{Freundlich isotherm } \ln q_e = \ln K_F + \frac{1}{n} \ln C_e \tag{10}$$

$$\text{Langmuir isotherm } \frac{C_e}{q_e} = \frac{C_e}{q_m} + \frac{1}{K_L q_m} \tag{11}$$

where K_F is Freundlich constant (l/mg), $1/n$ is the heterogeneity factor, K_L is the Langmuir adsorption constant (l/mg) related to energy of adsorption and q_m signifies adsorption capacity (mg/g).

Figs. 10 and 11 show the Freundlich ($\ln q_e$ versus $\ln C_e$) and Langmuir (C_e/q_e versus C_e) plot, respectively, for the removal of OG and MV with BFA at 30 °C. The data have been analysed by two correlation coefficients. The linear R^2 coefficients for the linearised plots shown in Fig. 11 and 12 are all above 0.9147 (Table 3). The non-linear R^2 values are based on the actual deviation between the experimental points and the theoretically predicted data points and are a better correlation of experimental data. The non-linear correlation coefficients for the Freundlich and Langmuir isotherm analyses are shown in Table 3 and are all greater than 0.9564. In all cases the Freundlich equation represents a better fit of experimental data than the Langmuir

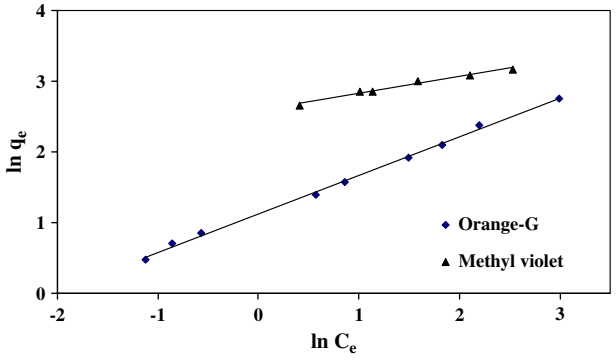

Fig. 11. Freundlich isotherm plots for the removal of dyes by BFA (temperature = 30 °C, contact time = 240 min).

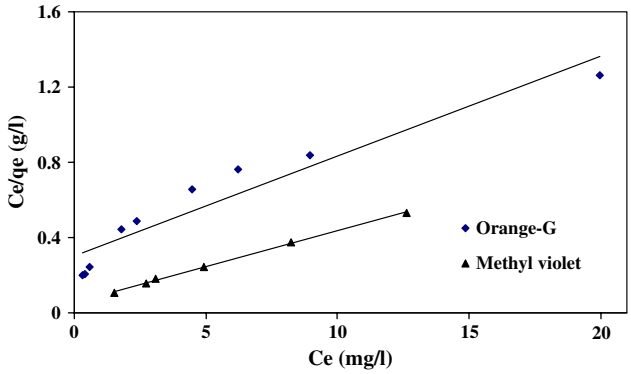

Fig. 12. Langmuir isotherm plots for the removal of dyes by BFA (temperature = 30 °C, contact time = 240 min).

equation. The values of parameters for Freundlich and Langmuir isotherms are given in Table 3. Similar results have been reported for adsorption of OG on chitosan (8); MV adsorption on bottom ash (48), and perlite (9). Values of $1/n$ less than 1 show the favourable nature of adsorption of OG and MV on BFA [65].

3.6.2. Redlich–Peterson (R–P) isotherm

Redlich and Peterson [66] incorporate three parameters into an empirical isotherm. The Redlich–Peterson isotherm has a linear dependence on concentration in the numerator and an exponential function in the denominator. It approaches the Freundlich model at high concentration and is in accordance with the low concentration limit of the Langmuir equation. Furthermore, the R–P equation incorporates three parameters into an empirical isotherm, and therefore, can be applied either in homogenous or heterogeneous systems due to the high versatility of the equation. It can be described as follows:

$$q_e = \frac{K_R C_e}{1 + a_R C_e^{\beta}} \tag{12}$$

where K_R is R–P isotherm constant (L/g), a_R is R–P isotherm constant (l/mg) and β is the exponent which lies between 1 and 0, where $\beta = 1$

$$q_e = \frac{K_R C_e}{1 + a_R C_e} \tag{13}$$

It becomes a Langmuir equation. Where $\beta = 0$

$$q_e = \frac{K_R C_e}{1 + a_R} \tag{14}$$

i.e. the Henry's Law equation.

Eq. (12) can be converted to a linear form by taking logarithms:

$$\ln\left(K_R \frac{C_e}{q_e} - 1\right) = \ln a_R + \beta \ln C_e \tag{15}$$

Table 3
Isotherm parameters for removal of dyes by bagasse fly ash

Freundlich constants					
Dye	K_F (mg/g)/(mg/l)$^{1/n}$		$1/n$	R_1^2 (linear)	R_2^2 (non-linear)
Orange-G	3.0836		0.5437	0.9977	0.9988
Methyl Violet	13.2964		0.2369	0.9830	0.9915
Langmuir constants					
Dye	K_L (l/mg)	q_m (mg/g)	R_L	R_1^2 (linear)	R_2^2 (non-linear)
Orange-G	0.1771	18.7960	0.3609	0.9147	0.9564
Methyl Violet	0.6804	26.2467	0.1281	0.9984	0.9915
Redlich–Peterson constants					
Dye	K_R (l/mg)	a_R	β	R_1^2 (linear)	R_2^2 (non-linear)
Orange-G	564.98	182.09	0.4583	0.9967	0.9984
Methyl Violet	41.09	2.35	0.8606	0.9994	0.9997
Dubnin–Radushkevich constants					
Dye	q_S (mg/g)		E (kJ/mol)	R_1^2 (linear)	R_2^2 (non-linear)
Orange-G	7.938		2.236	0.7775	0.8818
Methyl Violet	21.822		1.290	0.8572	0.9258
Tempkin constants					
Dye	K_T (l/mg)		B_1	R_1^2 (linear)	R_2^2 (non-linear)
Orange-G	3.3774		3.0697	0.8906	0.9437
Methyl Violet	16.6372		4.4618	0.9931	0.9965

Plotting the left-hand side of Eq. (14) against ln C_e to obtain the isotherm constants is not applicable because of the three unknowns, a_R, K_R and β. Therefore, a minimization procedure is adopted to solve Eq. (14) by maximizing the correlation coefficient between the theoretical data for q_e predicted from Eq. (14) and experimental data. Therefore, the parameters of the equations were determined by minimising the distance between the experimental data points and the theoretical model predictions with the solver add-in function of the Microsoft excel.

The linearised form of the R–P isotherm plots for the sorption of the OG and MV dyes onto BFA are presented in Fig. 13. The R–P isotherm constants a_R, K_R and β and the correlation coefficients, R^2, for the R–P isotherm are listed in Table 3. The correlation coefficients are significantly higher than the Langmuir isotherm R^2 values for both OG and MV adsorption on BFA. However, in comparison with R^2 values for Freundlich isotherm fit, Redlich–Peterson isotherm shows better fit for MV adsorption only and trend is reverse in case of OG adsorption.

3.6.3. Dubinin and Radushkevich isotherm

Another equation used in the analysis of isotherms was proposed by Dubinin and Radushkevich [67].

$$q_e = q_s \exp(-B\varepsilon^2) \tag{16}$$

where q_s is D–R constant and ε can be correlated:

$$\varepsilon = RT \ln\left(1 + \frac{1}{C_e}\right) \tag{17}$$

The constant B gives the mean free energy E of sorption per molecule of sorbate when it is transferred to the surface of the solid from infinity in the solution and can be computed using the following relationship [68]:

$$E = \frac{1}{\sqrt{2B}} \tag{18}$$

Calculated Dubinin–Radushkevich constants for the adsorption of OG and MV on BFA are shown in Table 3,

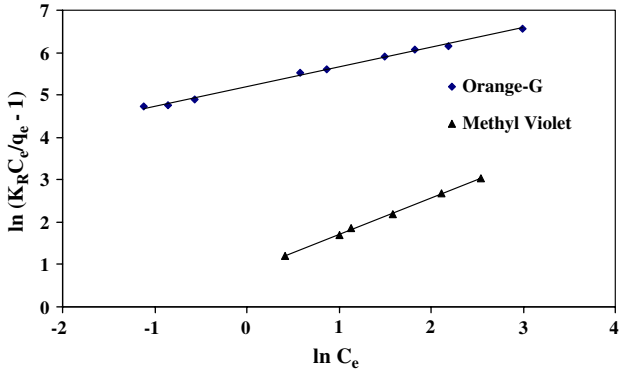

Fig. 13. Redlich-Petersen plot for the removal of dyes by BFA (temperature = 30 °C, contact time = 240 min).

the D–R isotherms are plotted against the experimental data points, as shown in Fig. 14. From this figure, it is clear that the sorption energy value is lowest for adsorption of MV on BFA. The values of correlation coefficients are much lower than the other four isotherms values. In all cases, the D–R equation represents the poorer fit of experimental data than the other isotherm equation.

3.6.4. Tempkin isotherm

Tempkin isotherm contains a factor that explicitly takes into account adsorbing species–adsorbate interactions. This isotherm assumes that: (i) the heat of adsorption of all the molecules in the layer decreases linearly with coverage due to adsorbate–adsorbate interactions, and (ii) adsorption is characterized by a uniform distribution of binding energies, up to some maximum binding energy [69]. Tempkin isotherm is represented by following equation:

$$q_e = \frac{RT}{b}\ln(K_t C_e) \tag{19}$$

Eq. (19) can be expressed in its linear form as:

$$q_e = B_1 \ln K_t + B_1 \ln C_e \tag{20}$$

where

$$B_1 = \frac{RT}{b} \tag{21}$$

The adsorption data can be analysed according to Eq. (20). A plot of q_e versus $\ln C_e$ enables the determination of the isotherm constants K_t and B_1. K_t is the equilibrium binding constant (l/mol) corresponding to the maximum binding energy and constant B_1 is related to the heat of adsorption. This isotherm is plotted in Fig. 15 for OG and MV adsorption on BFA and values of the parameters are given in Table 3.

Analysis of R^2 (non-linear) values from Table 3 shows that Freundlich equation is found to best represent the equilibrium data for OG-BFA system while Redlich–Peterson equation better fits the data for MV-BFA system. Fig. 16 depicts the comparison of experimental and predicted amount of OG adsorbed on BFA for all the isotherm models studied.

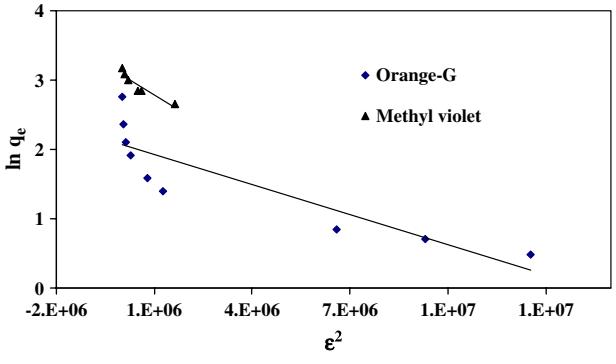

Fig. 14. Dubnin-Reduskevich isotherm plots for the removal of dyes by BFA (temperature = 30 °C, contact time = 240 min).

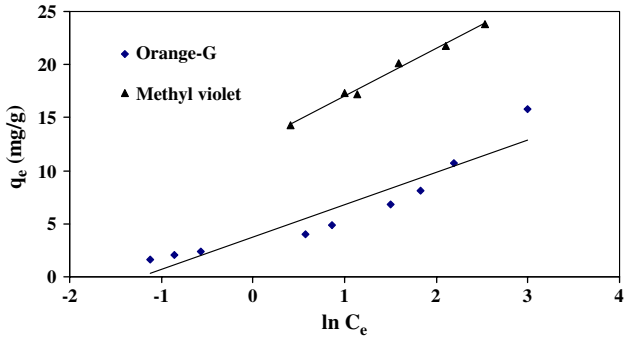

Fig. 15. Tempkin isotherm plots for the removal of dyes by BFA (temperature = 30 °C, contact time = 240 min).

3.7. Thermodynamic study

Thermodynamic data such as adsorption energy can be obtained from Langmuir and Tempkin equation [70].

$$-\Delta G^0_{ads} = RT\ln(K) \tag{22}$$

where K is constant. For the Langmuir isotherm, the Gibbs free energy of adsorption for OG and MV adsorption on BFA as calculated from Langmuir constant was found to be −28.46, −31.11 and −31.50 kJ/mol, respectively. Thus adsorption of MV (with a more negative value) is more favoured although other dyes have comparable values. From constant K_t (Table 3), the Gibbs free energies of adsorption for OG and MV adsorption on BFA were found to be −35.89 and −39.52 kJ/mol, respectively. Interestingly, adsorption of MV, again, has more negative values and thus, is more favoured.

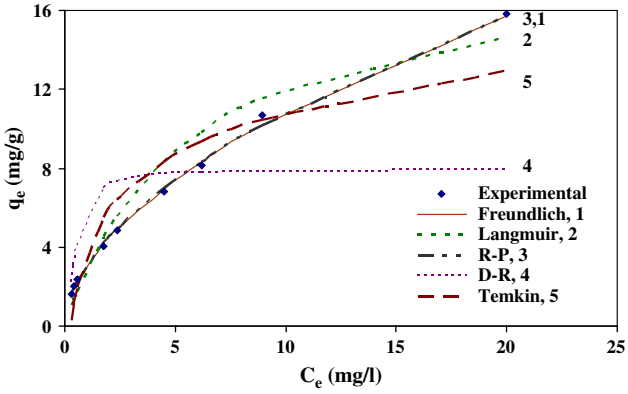

Fig. 16. Equilibrium isotherms for Orange-G adsorption on BFA.

3.8. Error analysis

Due to the inherent bias resulting from linearisation, five different error functions of non-linear regression basin were employed in this study to evaluate the isotherm constants.

3.8.1. The sum of the squares of the errors (SSE)

This most commonly used error function has one major drawback. The function will result in the calculated isotherm parameters providing a better fit at the higher end of the liquid phase concentration range. This is because the magnitude of the errors and hence the square of the errors will increase as concentration increases.

$$\sum_{i=1}^{n} \left(q_{e,calc} - q_{e,meas}\right)_i^2 \tag{23}$$

3.8.2. The sum of the absolute errors (SAE)

Isotherm parameters determined using this method would provide a better fit as the magnitude of the errors increase, biasing the fit towards the high concentration data.

$$\sum_{i=1}^{n} \left|q_{e,calc} - q_{e,meas}\right|_i \tag{24}$$

3.8.3. The average relative error (ARE) [71]

This error function attempts to minimise the fractional error distribution across the entire concentration range.

$$\frac{100}{n}\sum_{i=1}^{n} \left|\frac{\left(q_{e,meas} - q_{e,calc}\right)}{q_{e,meas}}\right|_i \tag{25}$$

3.8.4. The hybrid fractional error function (HYBRID)

This error function was developed [72] in order to improve the fit of the SSE method at low concentration values by dividing by the measured value. In addition a divisor was included as a term for the number of degrees of freedom for the system – the number of data points n minus the number of parameters p within the isotherm equation.

$$\frac{100}{n-p}\sum_{i=1}^{n} \left[\frac{\left(q_{e,meas} - q_{e,calc}\right)}{q_{e,meas}}\right]_i \tag{26}$$

3.8.5. Marquardt's percent standard deviation (MPSD)

This error function [73] was used previously by a number of researchers in this field [8,74,75]. It is similar in some aspects to a geometric mean error distribution modified according to the number of degrees of freedom of the system.

$$100\sqrt{\frac{1}{n-p}\sum_{i=1}^{n} \left(\frac{\left(q_{e,meas} - q_{e,calc}\right)}{q_{e,meas}}\right)_i^2} \tag{27}$$

3.8.6. Choosing best isotherm model

Since each of the error functions produce a different set of isotherm parameters, it is difficult to identify directly an overall optimum parameter set. Thus, a normalisation of each parameter is employed in order to have a better comparison between the parameter sets for the single isotherm model [8]. In the normalisation processes first each error function was selected in turn and the results for each parameter set were determined. Secondly, the errors determined for a given error function were divided by the maximum to obtain the normalised errors for each parameter set. Lastly, the normalised errors for each parameter set were summed. The values of all five error measurements were presented in Table 4. These values show that the Freundlich

Table 4
Values of five different error analyses of isotherm models of dyes on BFA

Isotherm	SSE	SAE	ARE	HYBRID	MPSD
Orange-G					
Freundlich	0.4203	1.4689	3.1638	−0.0406	4.0073
Langmuir	9.0683	8.2874	20.3533	4.1932	25.9051
R–P	0.4215	1.4857	3.1958	−0.0855	4.0294
D–R	90.6827	20.9117	43.1560	−32.5526	55.6470
Tempkin	19.3161	11.4380	29.8991	8.3406	42.2746
Methyl Violet					
Freundlich	1.0237	2.1855	1.9470	0.0228	2.6845
Langmuir	1.6588	2.6430	2.5584	0.7884	4.0634
R–P	0.3810	1.2142	1.0834	0.0180	1.6716
D–R	9.3908	6.4435	5.6696	0.5842	7.8366
Tempkin	0.4183	1.3564	1.2217	0.0435	1.7399

equation 'best-follows' the equilibrium data for OG adsorption on BFA whereas Redlich–Peterson isotherm best-fits for MV-BFA system. This is same as predicted by R^2 (non-linear) analysis.

4. Conclusion

The present study shows that bagasse fly ash (BFA) is an effective adsorbent for the removal of Orange-G (OG) and Methyl Violet (MV) from aqueous solution. Physico-chemical characteristics, surface area, pore volume and pore size observed exhibit potential use of BFA as adsorbent. Thermogravimetric analysis exhibited the thermal stability of BFA even at temperature up to 300 °C. The effective pH for OG and MV removal was 4 and 9, respectively. Higher percentage of OG and MV was removed by BFA provided the initial dye concentration was low in solution. Quasi-equilibrium was practically achieved in 4 h. Adsorption kinetics followed second-order rate expression with initial sorption rate being higher for MV adsorption on BFA. Error analysis showed that Freundlich isotherm best-fits equilibrium data for OG-BFA system whereas Redlich–Peterson isotherm best-follows the data for MV-BFA system. The results would be useful for the design of wastewater treatment plants for the removal of dye.

References

[1] Namasivayam C, Radhika R, Suba S. Uptake of dyes by a promising locally available agricultural solid waste: coir pith. Waste Manag 2001;21:381–7.
[2] Mishra G, Tripathy M. A critical review of the treatment for decolorization of textile effluent. Colourage 1993;40:35–8.
[3] Wong Y, Yu J. Laccase catalysed decolorisation of synthetic dyes. Water Res 1999;33(16):3512–20.
[4] Mckay G, Allen SJ, Meconney IF, Ottrburn MS. Transport processes in the sorption of colored ions by peat particles. J Colloid Interface Sci 1981;80(2):323–39.
[5] McKay G. Adsorption of dyestuffs from aqueous solutions with activated carbon I: equilibrium and batch contact-time studies. J Chem Technol Biotechnol 1982;32:759–72.
[6] McKay G, Otterburn MS, Sweeney AG. The removal of colour from effluent using various adsorbents – III silica: rate processes. Water Res 1980;14:15–20.
[7] McKay G, Blair HS, Gardner JR. Adsorption of dyes on chitin. I. Equilibrium studies. J Appl Polym Sci 1982;27:3043–57.
[8] Wong YC, Szeto YS, Cheung WH, McKay G. Adsorption of acid dyes on chitosan – equilibrium isotherm analyses. Process Biochem 2004;39:693–702.
[9] Dogan M, Alkan M. Adsorption kinetics of methyl violet onto perlite. Chemosphere 2003;50:517–28.
[10] El-Geundi MS. Homogeneous surface diffusion model for the adsorption of basic dyestuffs onto natural clay in batch adsorbers. Adsor Sci Technol 1991;8:217–25.
[11] El-Geundi MS. Branched-pore kinetic model for basic dyestuff adsorption onto natural clay. Adsor Sci Technol 1993;9(3):199–211.
[12] El-Geundi MS. Pore diffusion model for the adsorption of basic dyestuffs onto natural clay in batch adsorbers. Adsor Sci Technol 1993;9(2):109–20.
[13] Mckay G, El-Geundi M, Nassar MM. Equilibrium studies during the removal of dye stuffs from aqueous solutions using bagasse pith. Water Res 1987;21(12):1513–20.
[14] Mckay G, El-Geundi M, Nassar MM. External mass transport process during the adsorption of dyes onto bagasse pith. Water Res 1988;22(12):1527–33.
[15] Nassar MM, Ashour EA, Magdy YH. Dye adsorbent bagasse, a new potential source for energy conversion. In: Proceedings of the fifth international conference on energy and environment, Cairo, Egypt;1996. p. 993–1001.
[16] Mall ID, Upadhyay SN. Studies on treatment of basic dyes bearing wastewater by adsorptive treatment using fly ash. Ind J Environ Health 1998;40(2):177–88.
[17] Mall ID, Upadhyay SN. Removal of basic dyes from wastewater using boiler bottom ash. Ind J Environ Health 1995;37(1):1–10.
[18] Mall ID, Upadhyay SN. Treatment of methyl violet bearing wastewater from paper mill effluent using low cost adsorbents. J Indian Pulp Paper Technol Assoc 1995;7(1):51–7.
[19] Swamy MM, Mall ID, Prasad B, Mishra IM. Sorption characteristics of O-cresol on bagasse fly ash and activated carbon. Ind J Environ Health 1998;40(1):67–78.
[20] Poots VJP, McKay G, Healy JJ. Removal of basic dye from effluent using wood as an adsorbent. J Water Pollut Control Fed 1978;50:926–39.
[21] Asfour HM, Fadali OA, Nassar MM, El-Geundi MS. Equilibrium studies on adsorption of basic dyes on hardwood. J Chemical Tech Biotech 1985;35A:21–7.
[22] Asfour HM, El-Geundi MS, Fadali OA, Nassar MM. Colour removal from textile effuents using hardwood sawdust as an adsorbent. J Chemical Tech Biotech 1985;35A:28–35.
[23] Magdy YH. The adsorption of mixed dyes onto hardwood in fixed bed. Adsor Sci Technol 1996;13(5):367.
[24] Garg VK, Kumar R, Yadav AB, Gupta R. Dye removal from aqueous solution by adsorption on treated sawdust. Bioresour Technol 2003;89:121–4.
[25] Malik PK. Use of activated carbons prepared from sawdust and rice-husk for adsorption of acid dyes: a case study of acid yellow 36. Dyes Pigments 2003;56:239–49.
[26] Poots VJP, Mckay G, Healy JJ. The removal of acid dye from effluent using natural adsorbents I-peat. Water Res 1976;10:1061–6.
[27] Allen SJ. Equilibrium adsorption isotherms for peat. Fuel 1987;66:1171–6.
[28] Allen SJ, Mckay G, Khader KYH. Intraparticle diffusion of a basic dye during adsorption onto sphagnum peat. Environ Pollut 1989;56:39–50.
[29] El-Geundi MS. External mass transport processes during the adsorption of basic dyestuffs onto Maize Cob. Adsor Sci Technol 1990;7(3):124.
[30] Yehia HM, Abd El-Hakim AM. Adsorption of dyestuffs from aqueous solutions using bean-waste I. External mass transfer processes. J Egypt Soc Eng 1997;36(2):44.
[31] Namasivayam C, Kanchana N. Waste banana pith as adsorbent for colour removal from wastewaters. Chemosphere 1992;25:1691–705.
[32] Namasivayam C, Kanchana N, Yamuna RT. Waste banana pith as adsorbent for the removal of rhodamine-B from aqueous solution. Waste Manag 1993;13:89–95.
[33] Namasivayam C, Prabha D, Kumutha M. Removal of direct red and acid brilliant blue by adsorption on to banana pith. Bioresour Technol 1998;64:77–9.
[34] Namasivayam C, Dinesh Kumar M, Selvi K, Ashruffunissa Begum R, Vanathi T, Yamuna RT. 'Waste' coir pith – a potential

biomass for the treatment of dyeing wastewaters. Biomass Bioenergy 2001;21:477–83.
[35] Namasivayam C, Kavitha D. Removal of congo red from water by adsorption onto activated carbon prepared from coir pith, an agricultural solid waste. Dyes Pigments 2002; 54:47–58.
[36] Namasivayam C, Arasi DJSE. Removal of congo red from wastewater by adsorption onto waste red mud. Chemosphere 1997;34:401–17.
[37] Namasivayam C, Muniasamy N, Gayathri K, Rani M, Ranganathan K. Removal of dyes from aqueous solutions by cellulosic waste orange peel. Bioresour Technol 1996;57: 37–43.
[38] Namasivayam C, Yamuna RT. Removal of congo red from aqueous solutions by biogas waste slurry. J Chem Technol Biotechnol 1992;53:153–7.
[39] Namasivayam C, Yamuna RT. Removal of Rhodamine B by biogas residual slurry from aqueous solution. Water Air Soil Pollut 1992;65:101–9.
[40] Pollard SJT, Fowler GD, Sollars CJ, Perry R. Low-cost adsorbents for waste and wastewater wastewater treatment: a review. Sci Total Environ 1992;116:31–2.
[41] Mall ID, Upadhaya SN, Sharma YC. A review on economical treatment of wastewaters and effluents by adsorption. Int J Environ Stud 1996;51:77–124.
[42] Bailey SE, Olin TJ, Bricka RM, Adrian DD. A review of potentially low cost sorbents for heavy metals. Water Res 1999;33(11):2469–79.
[43] Mall ID, Mishra N, Mishra IM. Removal of organic matter from sugar mill effluent using bagasse flyash activated carbon. Res Indus 1994;39(6):115–9.
[44] Srivastava VC. Treatment of pulp and paper mill effluent. MTech dissertation, Indian Institute of Technology Roorkee, Roorkee, India; 2003.
[45] Mall ID, Tewari S, Singh N, Mishra IM. Utilisation of bagasse fly ash and carbon waste from fertiliser plant for treatment of pyridine and 3-picoline bearing wastewater. Proceeding of the eighteenth international conference on "solid waste technology and management", held at Philadelphia, PA, USA; March 23–26, 2003.
[46] Swamy MM, Mall ID, Prasad B. Resorcinol removal aqueous solution by bagasse fly ash and activated carbon. Inst Eng (India) J Environ 1997;77(2):49–54.
[47] Gupta VK, Jain CK, Ali I, Sharma M, Saini VK. Removal of cadmium and nickel from wastewater using bagasse fly ash – a sugar industry waste. Water Res 2003;37:4038–44.
[48] Gupta VK, Ali I. Utilisation of bagasse fly ash (a sugar industry waste) for the removal of copper and zinc from wastewater. Sep Purif Technol 2000;18:131–40.
[49] Gupta VK, Mohan D, Sharma S, Sharma M. Removal of basic dyes (rhodamine B and methylene blue) from aqueous solutions by bagasse fly ash. Sep Sci Technol 2000;35(13):2097–113.
[50] IS 1350 (part I). Methods of test for coal and coke (proximate analysis). New Delhi, India: Bureau of Indian Standards, Manak Bhawan; 1984.
[51] Puri BR, Walker PL, editors. Chemistry and physics of carbon. New York: Marcel Dekker; 1966. p. 161.
[52] Ng JCY, Cheung WH, McKay G. Equilibrium studies of the sorption of Cu(II) ions chitosan. J Colloid Interface Sci 2002;255:64–74.
[53] Panday KK, Prasad G, Singh VN. Mixed adsorbent for Cu(II) removal from aqueous solutions. Environ Technol Lett 1986;50(7):547–54.
[54] Inbraj BS, Sulochana N. Basic due adsorption on a low cost carbonaceous sorbent – kinetic and equilibrium studies. Indian J Technol 2002;9:201–8.
[55] Pedro Silva J, Sousa S, Rodrigues J, Antunes H, Porter JJ, Goncalves I, et al. Adsorption of acid orange 7 dye in aqueous solutions by spent brewery grains. Sep Purif Technol 2004;40:309–15.
[56] Jain AK, Gupta VK, Bhatnagar A, Suhas. A comparative study of adsorbents prepared from industrial wastes for removal of dyes. Sep Sci Technol 2003;38:463–81.
[57] Lagergren S. About the theory of so called adsorption of soluble substances. Ksver Veterskapsakad Handl 1898;24:1–6.
[58] Ho YS, McKay G. Pseudo-second order model for sorption processes. Process Biochem 1999;34:451–65.
[59] Aharoni C, Sideman S, Hoffer E. Adsorption of phosphate ions by collod ion-coated alumina. J Chem Technol Biotechnol 1979;29:404–12.
[60] Tutem E, Apak R, Unal CF. Adsorptive removal of chlorophenols from water by bituminous shale. Water Res 1998;32:2315–24.
[61] Weber Jr WJ, Morris JC. Kinetics of adsorption on carbon from solution. J Sanit Engg Div ASCE 1963;89(SA2):31–59.
[62] Kannan K, Sundaram MM. Kinetics and mechanism of removal of methylene blue by adsorption on various carbons – a comparative study. Dyes Pigments 2001;51:25–40.
[63] Freundlich HMF. Over the adsorption in solution. J Phys Chem 1906;57:385–471.
[64] Langmuir I. The adsorption of gases on plane surfaces of glass, mica and platinum. J Am Chem Soc 1918;40:1361–403.
[65] Faust SD, Aly OM. Adsorption processes for water treatment. Butterworths; 1987.
[66] Redlich O, Peterson DL. A useful adsorption isotherm. J Phys Chem 1959;63:1024–6.
[67] Dubinin MM, Radushkevich LV. Equation of the characteristic curve of activated charcoal. Chem Zentr 1947;1:875.
[68] Hasany SM, Chaudhary MH. Sorption potential of Hare river sand for the removal of antimony from acidic aqueous solution. Appl Radiat Isot 1996;47:467–71.
[69] Tempkin MJ, Pyzhev V. Acta Physiochim URSS 1940;12:217–22.
[70] Kim Y, Kim C, Choi I, Rengraj S, Yi J. Arsenic removal using mesoporous alumina prepared via a templating method. Environ Sci Technol 2004;38:924–31.
[71] Kapoor A, Yang RT. Correlation of equilibrium adsorption data of condensable vapours on porous adsorbents. Gas Sep Purif 1989;3(4):187–92.
[72] Porter JF, McKay G, Choy KH. The prediction of sorption from a binary mixture of acidic dyes using single- and mixed isotherm variants of the ideal adsorbed solute theory. Chem Eng Sci 1999;54:5863–85.
[73] Marquardt DW. An algorithm for least-squares estimation of nonlinear parameters. J Soc (Ind) Appl Math 1963;11:431–41.
[74] Seidel A, Gelbin D. On applying the ideal adsorbed solution theory to multicomponent adsorption equilibria of dissolved organic components on activated carbon. Chem Eng Sci 1988;43(1):79–89.
[75] Ng JCY, Cheung WH, McKay G. Equilibrium studies for the sorption of lead from effluents using chitosan. Chemosphere 2003;52:1021–30.